# Predicting wildfire occurrence distribution with spatial point process models and its uncertainty assessment: a case study in the Lake Tahoe Basin, USA

*Jian Yang*[A,B,C,H], *Peter J. Weisberg*[A], *Thomas E. Dilts*[A], *E. Louise Loudermilk*[D,G], *Robert M. Scheller*[D], *Alison Stanton*[E] *and Carl Skinner*[F]

[A]Department of Natural Resources and Environmental Science, University of Nevada, Reno, 1664 N. Virginia St. Mail Stop 186, Reno, Nevada 89557, USA.

[B]State Key Laboratory of Forest and Soil Ecology, Institute of Applied Ecology, Chinese Academy of Sciences, Shenyang 110164, P. R. China.

[C]Department of Forestry, TP Cooper Building, University of Kentucky, Lexington, KY, 40546, USA.

[D]Environmental Science and Management Department, Portland State University, PO Box 751, Portland, OR, 97207, USA.

[E]3170 Highway 50 Suite #7, South Lake Tahoe, CA, 96150, USA.

[F]Pacific Southwest Research Station, USDA Forest Service, 3644 Avtech Parkway, Redding, CA, 96002, USA.

[G]Present address: Forestry Sciences Laboratory, Center for Forest Disturbance Science, USDA Forest Service, 320 Green Street, Athens, GA 30602, USA.

[H]Corresponding author. Email: jian.yang@uky.edu

**Abstract.** Strategic fire and fuel management planning benefits from detailed understanding of how wildfire occurrences are distributed spatially under current climate, and from predictive models of future wildfire occurrence given climate change scenarios. In this study, we fitted historical wildfire occurrence data from 1986 to 2009 to a suite of spatial point process (SPP) models with a model averaging approach. We then predicted human- and lightning-caused wildfire occurrence over the 2010–2100 period in the Lake Tahoe Basin, a forested watershed in the western US with an extensive wildland–urban interface. The purpose of our research was threefold, including (1) to quantify the influence of biophysical and anthropogenic explanatory variables on spatial patterns of wildfire occurrence, (2) to model current and future spatial distribution of wildfire occurrence under two carbon emission scenarios (A2 and B1), and (3) to assess prediction uncertainty due to model selection. We found that climate variables exerted stronger influences on lightning-caused fires, with climatic water deficit the most important climatic variable for both human- and lightning-caused fires. The recent spatial distribution of wildfire hotspots was mainly constrained by anthropogenic factors because most wildfires were human-caused. The future distribution of hotspots (i.e. places with high fire occurrence density), however, was predicted to shift to higher elevations and ridge tops due to a more rapid increase of lightning-caused fires. Landscape-scale mean fire occurrence density, averaged from our top SPP models with similar empirical support, was predicted to increase by 210% and 70% of the current level under the A2 and B1 scenarios. However, individual top SPP models could lead to substantially different predictions including a small decrease, a moderate increase, and a very large increase, demonstrating the critical need to account for model uncertainty.

**Additional Keywords:** climatic water deficit, model uncertainty, multi-model inference, predictive modelling, spatial point process.

## Introduction

Wildfire activity has increased considerably across many terrestrial ecosystems in recent decades, partly due to climate warming (e.g. Flannigan *et al.* 2009; Kelly *et al.* 2013). It has been demonstrated that warming temperatures and earlier spring seasons are associated with a 4-fold increase in frequency of large forest wildfires in the western United States since 1986, compared with the period from 1970 to 1986 (Westerling *et al.* 2006). The increasing wildfire activity can cause degradation of ecosystem functions, create hazards for people and increase fire suppression costs (Stephens and Ruth 2005; Syphard *et al.* 2008). In order to effectively manage fuels and to reduce the risk

of large, severe fires, it is important to understand how wildfire occurrence and its spatial distribution may respond to ongoing climate change in the near future.

Many studies have found that the spatial distribution of wildfire occurrence is strongly patterned at landscape to regional scales (Bar Massada *et al.* 2011; Finney *et al.* 2011). It is determined by both top-down drivers reflecting broad-scale spatial variability of climate, and vegetation type and bottom-up drivers reflecting fine-scale spatial variability of fuel, topography and proximity to human ignition sources (Parisien and Moritz 2009). Comprehensive studies that examine how various controls influence wildfire occurrence are often conducted at regional or global scales with coarse spatial resolutions (e.g. Krawchuk *et al.* 2009; Wotton *et al.* 2010). However, planning of fuel treatments and modelling of fuel treatment effectiveness for reducing undesired fire behaviour and effects are often conducted at fine (1–10 ha) spatial resolutions (Finney 2007). Therefore, spatially explicit analysis of wildfire occurrence and its response to climate change at fine scales is warranted for assisting landscape-level fire and fuel management.

Spatial point process (SPP) modelling (Stoyan and Penttinen 2000) provides a promising approach for investigating wildfire occurrences at landscape scales (e.g. Podur *et al.* 2003; Yang *et al.* 2007; Juan *et al.* 2012). A SPP is any stochastic mechanism that generates the spatial point data – a collection of event (e.g. species presence, volcano eruption, fire occurrence) locations in a bounded region (Diggle 1983). The pattern of event locations often results from a mixture of both first-order and second-order effects. First-order effects (e.g. global spatial trends) are related to variation in the point intensity (i.e. mean number of events per unit area) of the spatial process; whereas second-order effects often result from local point interactions (Bailey and Gatrell 1995). SPP modelling involves fitting the location data to a spatial point process (e.g. Poisson, Cox) with two components, one quantifying first-order spatial covariate effects on the variation in the point intensity (e.g. Liu *et al.* 2012) and the other representing second-order point interaction effects (Baddeley and Turner 2000). SPP modelling offers a statistically rigorous framework for modelling presence-only data, as well as a set of tools for estimating likelihood function, choosing appropriate spatial resolution, and assessing goodness of fit (Diggle 1983; Warton and Aarts 2013). In the special case of the Poisson point process, SPP modelling is equivalent to MaxENT and logistic regression on randomly chosen pseudo-absences, but provides greater flexibility (Warton and Shepherd 2010; Renner and Warton 2013).

Early SPP applications of wildfire occurrences were exploratory, seeking mainly to discern spatial patterns such as regularity, clustering and randomness (e.g. Podur *et al.* 2003). Recently, SPP modelling has been used to quantify influences of various controls that drive these spatial patterns (e.g. Yang *et al.* 2007; Juan *et al.* 2012; Mundo *et al.* 2013) and to predict the response of wildfire occurrence to future climate conditions (e.g. Liu *et al.* 2012). Most SPP applications use a stepwise model selection approach to find a single best model. Due to reliance on a single model, parameter estimates and predictions of future responses lack consideration of model uncertainty (Whittingham *et al.* 2006). Multi-model inference approaches,
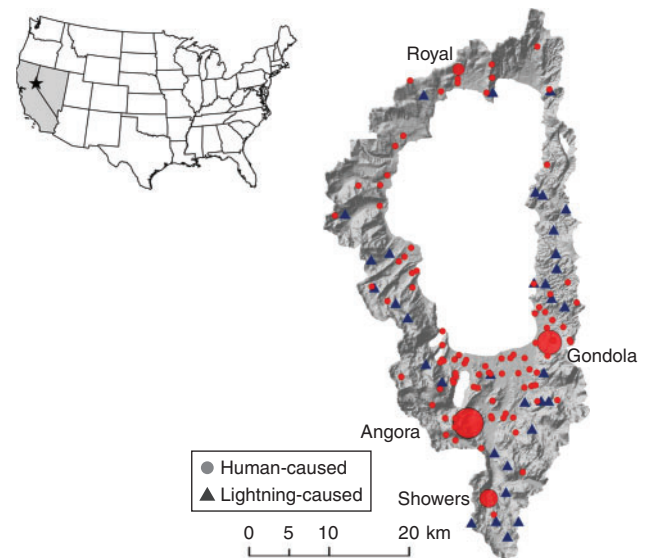


**Fig. 1.** Study area of the Lake Tahoe Basin with reported human- and lightning-caused fires greater than 0.1 ha in size between 1986 and 2009. The four largest fires (Angora, Gondola, Showers and Royal), all of which were human-caused, are shown in large circles.

often involving model averaging, can be more informative than the traditional stepwise modelling approach in that several models can be ranked and weighted to provide a quantitative measure of relative support for each competing model (Grueber *et al.* 2011). Model averaging, which can provide a robust means of obtaining parameter estimates and making predictions, is now increasingly used in the analysis of ecological data when coupled with generalised linear models (GLM; Burnham and Anderson 2002). However, model averaging has not been applied in the SPP analysis of wildfire occurrences.

In this study, we integrated SPP within a model averaging approach to examine the drivers and responses of wildfire occurrences to potential climate change in the LTB, a western US forest watershed with an extensive wildland–urban interface (WUI) where the threat of catastrophic wildfire to human lives and structures, as well as to natural resources is a major concern. Our study used SPP modelling to address the following questions: (1) What are the environmental influences on wildfire occurrence patterns in the LTB? (2) What is the potential response of wildfire occurrence to climate change? and (3) To what extent can model averaging be used to bracket prediction uncertainty?

## Methods

### Study area

The Lake Tahoe Basin (LTB; 39°4′12″N, 120°0′0″W) is located in the northern Sierra Nevada of California and Nevada, USA (Fig. 1). The LTB consists of 49 600 ha of Lake Tahoe itself and 83 000 ha of terrestrial habitats and urban areas. More than 75% of LTB land is managed by the Lake Tahoe Basin Management Unit (LTBMU) of the US Forest Service. The climate in LTB is characterised by warm dry summers and cold wet winters. Most (80%) precipitation falls as snow during the winter. Mean monthly temperatures at South Lake Tahoe (elevation 1820 m)

range from −1°C in January to 19°C in July, and mean annual precipitation is 784 mm. The terrain is complex and steep, with elevation ranging from less than 1800 m to 3315 m. Natural vegetation in the LTB is dominated by coniferous forest, with Jeffrey pine (*Pinus jeffreyi*)–white fir (*Abies concolor*), red fir (*A. magnifica*)–western white pine (*P. monticola*), and lodgepole pine (*P. contorta* var. *murrayana*)–whitebark pine (*P. albicaulis*) forests respectively dominating at lower montane (1900–2000 m), upper montane (2000–2300 m) and subalpine (>2300 m) zones (Taylor 2004).

Prior to European settlement, fires in the LTB were ignited by lightning or by Native Americans of the Washoe tribe (Taylor and Beaty 2005). The fire return interval (FRI) during the pre-settlement period (1650–1850) varied throughout the entire Basin, but fire return intervals were mostly short (5–20 years) in Jeffrey pine-dominated forests widely distributed at the lowest elevations around the lake and in the south (Taylor and Beaty 2005). The modern (1850–2000) fire regime has changed from one dominated by frequent low-intensity fires to infrequent high-intensity fires due to strong fire suppression and fuel build-up after massive logging that occurred between 1873 and 1900 (Taylor 2004). Active fire exclusion since the beginning of the 20th century has nearly eliminated wildfires in the LTB, with less than 20% of the LTB forests having burned since 1910 (Safford *et al.* 2009).

*Fire data*

Historical fire occurrence data (1949–2009) were acquired from the US Forest Service (USFS) Region 5 Geospatial Data Portal (http://www.fs.usda.gov/detail/r5/landmanagement/gis/?cid=STELPRDB5327833, accessed 19 June 2012). The fire occurrence data contained information on fire start location, cause, date of occurrence and fire size. Although the database contained fires reported as early as 1949 in LTB, we chose year 1986 as the early cut-off date because this is when many agencies began reporting fire start location as points (latitude–longitude) rather than as within an area (township, range section). After removing a small proportion (5%) of erroneous records due to duplicates and inaccurate locations, we obtained 1340 fire occurrence records in LTB reported between 1986 and 2009. Fire season typically starts in May and ends in November with peaks in July and August. Among those fires, only 142 had a fire size greater than 0.25 acres (0.10 ha), a commonly used threshold for excluding small fires from further statistical analysis in the USFS (e.g. Miranda *et al.* 2012). Those extremely small fires that were often suppressed on initial attack were excluded from our analysis because they not only contributed little in total area burned, but also adversely affected our SPP modelling performance as we lacked GIS variables with adequately high spatial resolution to capture such fine-scale influences of fire suppression activity on the landscape. Of the 142 fires used in our analysis, ∼76% were human-caused and 24% were lightning-caused. Only four fires (Fig. 1) were larger than 100 ha: the Angora Fire (burned in late June 2007; 1250 ha), the Gondola Fire (early July 2002; 272 ha), the Showers Fire (mid-August 2002; 119 ha) and the Royal Fire (mid-November 2003; 109 ha). These were all human caused and primarily burned in conifer forest dominated by Jeffrey pine and white fir at lower elevations (Safford *et al.* 2009).

*Guiding hypotheses and predictor variables*

Spatial patterns of wildfire occurrence over large landscapes and long periods are driven by ignition sources and availability of suitable biophysical conditions, including topography, vegetation and climate (Krawchuk and Moritz 2011). For lightning-caused wildfire, we hypothesised that lightning strike density was a major determinant of ignition source and positively associated with wildfire occurrence. For human-caused wildfire, we hypothesised that spatial distribution of roadways and population, which determines human accessibility to the LTB forest, was a major influence on wildfire occurrence. However, because human accessibility could also facilitate fire suppression efforts, we expected that its influences on wildfire occurrence would not be monotonically positive.

We obtained a GIS database of lightning strike density for 1990–2009 from the National Lightning Detection Network (Vaisala Global Atmospherics 2012) to model the effects of lightning strike distribution on spatial patterns of lightning-caused wildfire occurrence (Fig. 2). We included distance to nearest road, road density and population density as predictor variables to represent human accessibility effects on ignition source (Table 1). Both road network and human population data were obtained from 2000 US Topologically Integrated Geographic Encoding and Referencing system (TIGER) Line files (US Census 2000, available at https://www.census.gov/geo/maps-data/data/tiger-line.html, verified 31 October 2014) and then processed using a GIS.

We hypothesised that topography influences the likelihood of fire occurrence because it can directly constrain human accessibility and lightning distribution, affect local climate, provide fire breaks, and indirectly affect fuel moisture, vegetation distribution and relative humidity (Rothermel 1983; Syphard *et al.* 2008). In addition to commonly used terrain variables such as elevation and slope, we included the Heat Load Index (HLI), Topographical Position Index (TPI) and Vector Ruggedness Measure (VRM). HLI describes potential heat load based on latitude, slope steepness and aspect (McCune and Keon 2002). VRM is a topographical roughness index that measures the three-dimensional dispersions of vectors orthogonal to the land surface (Sappington *et al.* 2007) and for purposes of our study is an indicator of human accessibility. VRM values in the output raster can range from 0 (no terrain variation) to 1 (maximum terrain variation). The TPI determines the relative position of a grid cell compared with its neighbours (Weiss 2001) and can be used to determine whether a cell is more likely to be located along a ridge (high TPI values) or in a valley bottom (low TPI values). TPI is dependent on the neighbourhood search radius; and we calculated TPI using a 1-km neighbourhood search radius after a preliminary comparison of explanatory power across systematically varying neighbourhood sizes.

Vegetation was also hypothesised to be an important control because different vegetation types can be related to different fuel types. We used a categorical vegetation map to represent different fuel types in LTB based on the USFS Fuel Characteristic Classification System (FCCC, http://www.fs.fed.us/pnw/fera/fccs/, accessed 19 October 2012). FCCC describes fuel beds in six strata including canopy, shrubs, nonwoody fuels, woody fuels, litter–lichen–moss and ground fuels (litter and duff). To represent
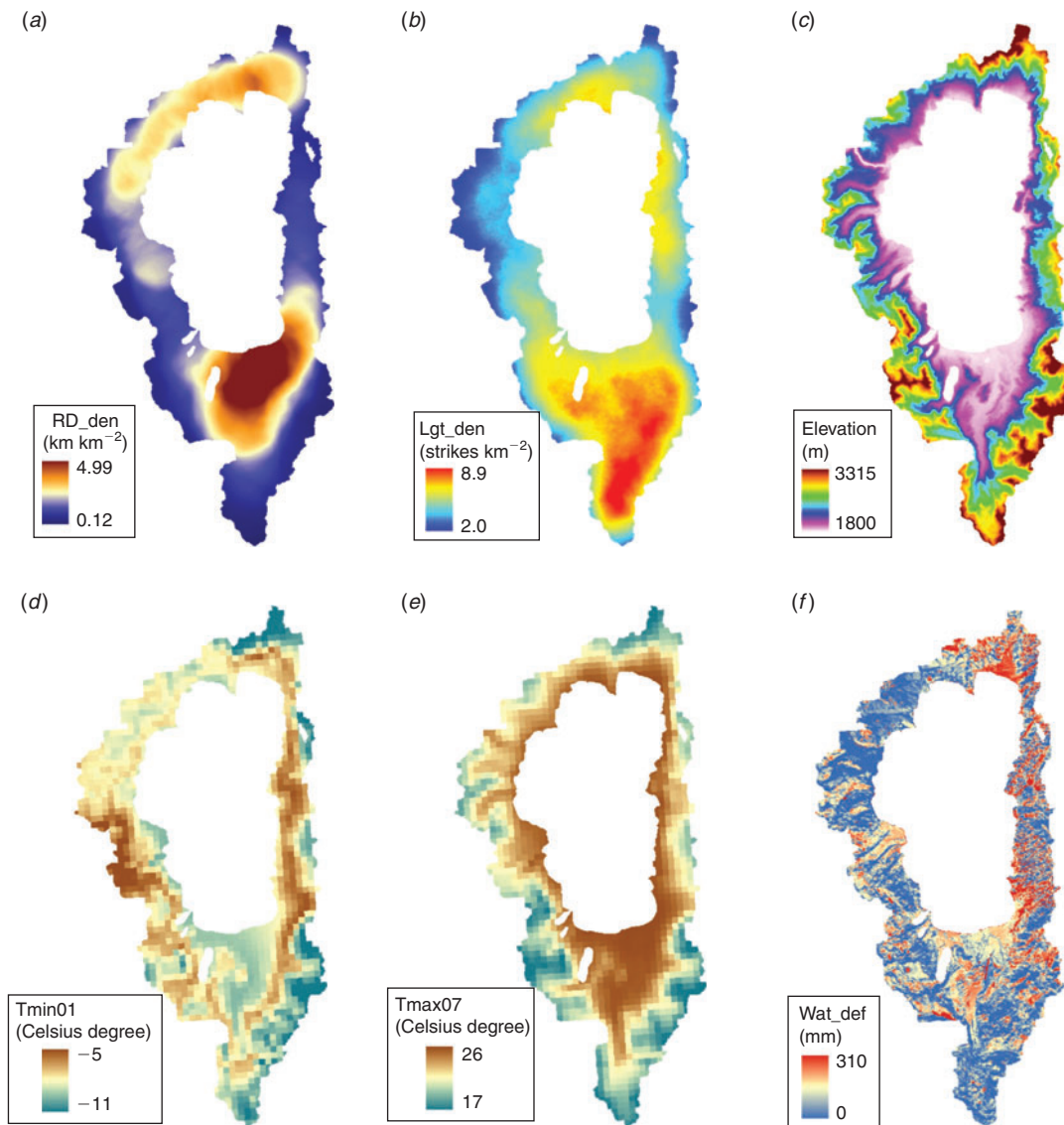
**Fig. 2.** Road density (*a*), lightning density (*b*), elevation (*c*), average January minimum temperature (*d*), average July maximum temperature (*e*), and annual water deficit (*f*) in the Lake Tahoe Basin.

broad-scale influences of vegetation on fire occurrence, we aggregated 74 fine-scale fuel types for the LTB into five vegetation types: conifer forest, deciduous forest, meadow, shrubland and miscellaneous vegetation. We also tried a finer aggregation scheme that divided conifer forest into several sub-types based on the fact that Jeffrey pine at lower elevations tends to be more readily available to burn than lodgepole pine at higher elevations. But in the end we still chose the broad scheme in the modelling to alleviate multicollinearity influences as the finer classification scheme was strongly correlated with elevation.

We used PRISM 30-year (1971–2000) average July maximum temperature, average January minimum temperature, mean July precipitation and mean January precipitation (PRISM 2007) to represent the effect of climate on vegetation productivity, rate of fuel accumulation and fuel moisture content (Whelan 1995). The 30-year means were used instead of annual

climatic variables because the spatial patterns of fire occurrence were modelled for the entire 24-year period from 1984 to 2009, not on an annual basis. We chose climatic variables from January and July because these two months were climatologically important for vegetation phenology and fire seasonality in the LTB, where the wildfire season peaks in July. In addition, a water balance metric – annual climatic water deficit (Stephenson 1998; Lutz *et al.* 2010) – was computed to represent water stress that vegetation might experience and considered an indirect proxy for fuel moisture. Climatic water deficit was calculated as the difference between potential and actual evapotranspiration. Actual evapotranspiration was calculated using a Thornthwaite approach (Thornthwaite and Mather 1955) in which temperature and precipitation were the primary climatic drivers. The effect of topography was incorporated by using HLI (McCune and Keon 2002; Lutz *et al.* 2010) as a modifier to

**Table 1.    Predictor variable datasets and sources**

| Variable | Abbreviation | Data source | Units |
|---|---|---|---|
| **Ignition sources** | | | |
| Distance to nearest road[§] | Dist_Rd | Derived from TIGER street map (https://www.census.gov/geo/maps-data/data/tiger-line.html, verified 31 October 2014) | metre |
| Road density[§] | Rd_Den | Derived from TIGER street map (https://www.census.gov/geo/maps-data/data/tiger-line.html, verified 30 October 2014) | km km$^{-2}$ |
| Population density[§] | Pop_Den | | people km$^{-2}$ |
| Lightning density[‡] | Lgt_Den | National Lightning Detection Network (http://www.vaisala.com/en/products/thunderstormandlightning detectionsystems/Pages/NLDN.aspx, verified 30 October 2014) | strikes km$^{-2}$ |
| **Topography and vegetation** | | | |
| Elevation | Elev | USGS National Elevation Dataset (http://ned.usgs.gov/, verified 03 October 2014) | metre |
| Slope | Slope | Derived from elevation | degree |
| Heat Load Index | HLI | McCune and Keon (2002) | unitless |
| Topographic Position Index | TPI | Weiss (2001) | metre |
| Vector Ruggedness Measure | VRM | Sappington *et al.* (2007) | unitless |
| Vegetation type | Veg | USFS Fuel Characteristic Classification System (http://www.fs.fed.us/pnw/fera/fccs/, verified 30 October 2014) | Categorical |
| **Climate** | | | |
| Maximum July temperature | Tmax07 | PRISM (2007) | °C |
| Minimum January temperature | Tmin01 | PRISM (2007) | °C |
| Mean July precipitation | Prep07 | PRISM (2007) | mm |
| Mean January precipitation | Prep01 | PRISM (2007) | mm |
| Annual climatic water deficit | Wat_Def | Stephenson (1998); Lutz *et al.* (2010) | mm |

[§]Excluded from the modelling of lightning-caused wildfire occurrence.
[‡]Excluded from the modelling of human-caused wildfire occurrence.

potential evapotranspiration. Following the approach of Lutz *et al.* (2010), a snowpack component and a soil moisture component were included in the model to account for storage of water that would occur during the winter and spring months. Climatic water deficit can be an important predictor of plant distributions (Stephenson 1998) and wildfire probability (Parisien *et al.* 2012).

All model predictor variables describing ignition source, topography, vegetation and climate patterns were only included if their pairwise Pearson correlations were moderate ($|r| < 0.6$) in order to avoid potential multicollinearity effects. In addition, these variables were projected and scaled to 100-m resolution GIS raster data with the same geographic extent, for the purpose of SPP modelling.

*Spatial point process modelling*

We modelled human- and lightning-caused wildfire occurrences separately using the SPP modelling technique. The point process models fitted to the data are often formulated in terms of their Papangelou conditional density $\lambda(u; x)$, which may be loosely interpreted as the conditional probability of having an event at a point $u$ given that the rest of the point process coincides with x (Baddeley and Turner 2000).

We modelled our wildfire occurrence data using an inhomogeneous Poisson point process, in which the conditional density function is the same as the density function $\lambda(u; \mathbf{x}) = \lambda(u)$ because spatial locations are independent of one another and so their interactions are not considered. The *intensity function*

(often called *density function* in SPP applications) of a Poisson point process is specified through a log–linear regression model as follows:

$$\lambda(u) = \exp(\theta_0 + \theta_1{}^*V_1 + \ldots + \theta_n{}^*V_n) \tag{1}$$

where $\lambda(u)$ is density at point $u$, which may be interpreted as the number of events that occurred per spatio–temporal unit. The $V_1 \ldots V_n$ are spatial covariates (i.e. predictor variables), and $\theta$ is the parameter vector ($\theta_0$, $\theta_1$, ..., $\theta_n$) to be estimated for the spatial covariates. The density $\lambda(u)$ will depend on $\theta$ to reflect anisotropy ('spatial trend', the change in density across the region of observation) or dependence on a covariate. The parameter vector $\theta$ was estimated via a maximum likelihood algorithm (Baddeley and Turner 2000) implemented in the *ppm* function of the 'Spatstat' package in the statistical computing software *R*.

*Model averaging*

Instead of finding a single best SPP model, we employed a model averaging approach that accounted for model selection uncertainty in order to obtain robust estimates of parameters ($\theta$) and model predictions (Johnson and Omland 2004). We included all predictor variables (Table 1) in the trend term of the log–linear regression model. The included continuous variables were transformed with a polynomial function (up to a power of two) to capture curvilinear effects. We then used all combinations of the predictor variables and their transformations to

construct a wide set of alternative models. Each model was fitted to the data and its Akaike Information Criterion (AIC) score was computed. The model with the smallest AIC score was used as a reference model, and the difference in AIC scores between each model and the reference model was also computed as the delta AIC ($\Delta$). A subset of fitted models with delta AIC <4 – a moderate threshold value recommended by Burnham and Anderson (2002) – was identified as including the best candidate models to be used in further model averaging steps.

For each candidate model, its Akaike weight was calculated as follows:

$$W_i = \frac{\exp(-1/2\Delta_i)}{\sum_{j=1}^{R} \exp(-1/2\Delta_j)}$$

where $W_i$ is the Akaike weight of the $i$th candidate model, $R$ is the total number of candidate models used in the model averaging and $\Delta$ is the delta AIC. The Akaike weight describes the relative likelihood of the model given the data and is thus an explicit measure of model support. The Akaike weight was used to compute the weighted average of parameter estimates and model predictions.

To quantify the relative importance of predictor variables, the sum of the Akaike weights over all of the models in which the parameter of interest appears was computed for each predictor variable (Johnson and Omland 2004). This measure was further normalised so that the sum of all predictor variables' relative importance was a mathematical unity. We also computed the weighted average of parameter estimates for each predictor variable and plotted a response function against the full range of the predictor variable based on such parameter estimates to quantify its partial influences on wildfire occurrence.

### Predicting wildfire occurrence distribution

Predicting wildfire occurrence distribution included two steps: (1) for each candidate SPP model, computing wildfire occurrence density at each raster cell based on the corresponding parameters and values of predictor variables; and (2) calculating Akaike weight-based average density across all candidate SPP models. Because such prediction across all cells was computationally intensive, we only selected the top 30 candidate SPP models for estimating predictive fire occurrence density maps. The differences in AICs among the top 30 SPP models for both lightning-caused and human-caused wildfire cases were around 2, which is often used as a strict threshold for choosing a subset of candidate models in the model averaging framework (Burnham and Anderson 2002).

We adopted the above approach in estimating separate maps for human- and lightning-caused wildfire occurrence density, and then summed the two maps to obtain a total wildfire density map. All maps had a spatial resolution of 100 m, which is consistent with the predictor GIS raster data, with a standardised unit of wildfire count per 100 km$^2$ per decade. In this study, we predicted historical and future wildfire occurrence distribution by holding all other predictor variables (i.e. ignition source, topography and vegetation) constant and allowing changes in climatic variables (i.e. temperature, precipitation and climatic water deficit) derived from future climate data under various climate change scenarios.

Future climate data were based on the projections of the CCCMA (Canadian Centre for Climate Modelling and Analysis) under both the A2 and B1 Special Report on Emissions Scenarios (SRES) AR4 carbon emission scenarios. The A2 scenario represents high $CO_2$ concentration ($\sim$850 ppm at the end of 21st century) due to high population size and slow technological adaptations, whereas the B1 scenario represents a less extreme $CO_2$ increase ($\sim$550 ppm) due to global integration of climate adaptations and introduction of resource-efficient technologies. Future climate data were also rescaled to 100-m spatial resolution using a bias correction delta down-scale approach (Maurer 2007). Because the climatic variables used in the model-building process were obtained from the 30-year average PRISM data, we also computed 30-year average climatic variables from the future climatic data to predict wildfire occurrence over four periods (1981–2010, 2011–2040, 2041–2070 and 2071–2100). The predicted historical and future wildfire occurrence distributions were compared in terms of landscape-level total wildfire occurrence density, proportion of lightning-caused wildfire occurrences and spatial patterns.

### Results

The relative importance of spatial controls of lightning- and human-caused wildfire occurrences in LTB varied greatly. The six most important predictor variables of lightning-caused wildfires, in decreasing order, were annual water deficit, elevation, lightning density, January minimum temperature, topographic position index and January precipitation. Topography and ignition agents contributed three of the top six important variables, as did climate variables. In contrast, variables describing human ignition agents (road density, population density and distance to road) and topography (HLI and VRM) contributed five of the top six important variables for human-caused fires. Only one climate variable (annual water deficit) was identified as a top variable for human-caused wildfires (Fig. 3).

Climatic water deficit exerted strong positive effects on both lightning- and human-caused wildfire occurrence, suggesting higher wildfire occurrence density in dry areas and periods. With other important influences held constant, lightning-caused wildfire occurrence density generally increased with elevation, but then gradually decreased after reaching an optimal elevation band, partly due to cooler temperatures and moister conditions at higher elevations. Lightning-caused wildfires were often found at ridge tops with high TPI values and in places with high lightning strike density (Fig. 3a). Human-caused wildfire density exhibited a positive association with road density, as higher road density indicates greater accessibility by humans. However, our modelling showed that other measures of human accessibility could exert curvilinear or even negative effects through their influences on fire suppression success rate and forest fire management policies. For example, human-caused wildfire occurrence density was initially higher in places closer to roads, decreased with increasing distance to road as human-caused ignitions became less likely, but then increased in places further away from roads that were more difficult to detect and access for fire suppression (Fig. 3b).

Predictions of mean fire occurrence density by the end of the 21st century varied greatly among the top 30 SPP models
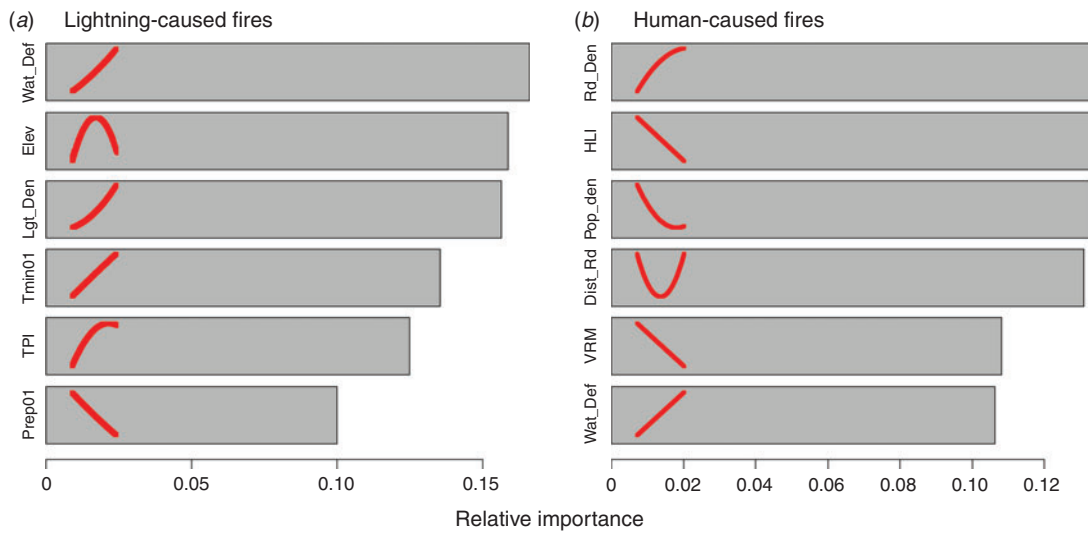
**Fig. 3.** The relative importance (length of grey bars denoting weighted relative frequency of being included within the set of best models) and marginal effects (red trend lines within each bar) of the six most important predictor variables for modelling spatial patterns of lightning-caused wildfire occurrence (*a*) and human-caused wildfire occurrence (*b*) in the Lake Tahoe Basin. Abbreviations of predictor variables and their corresponding full names are described in Table 1.
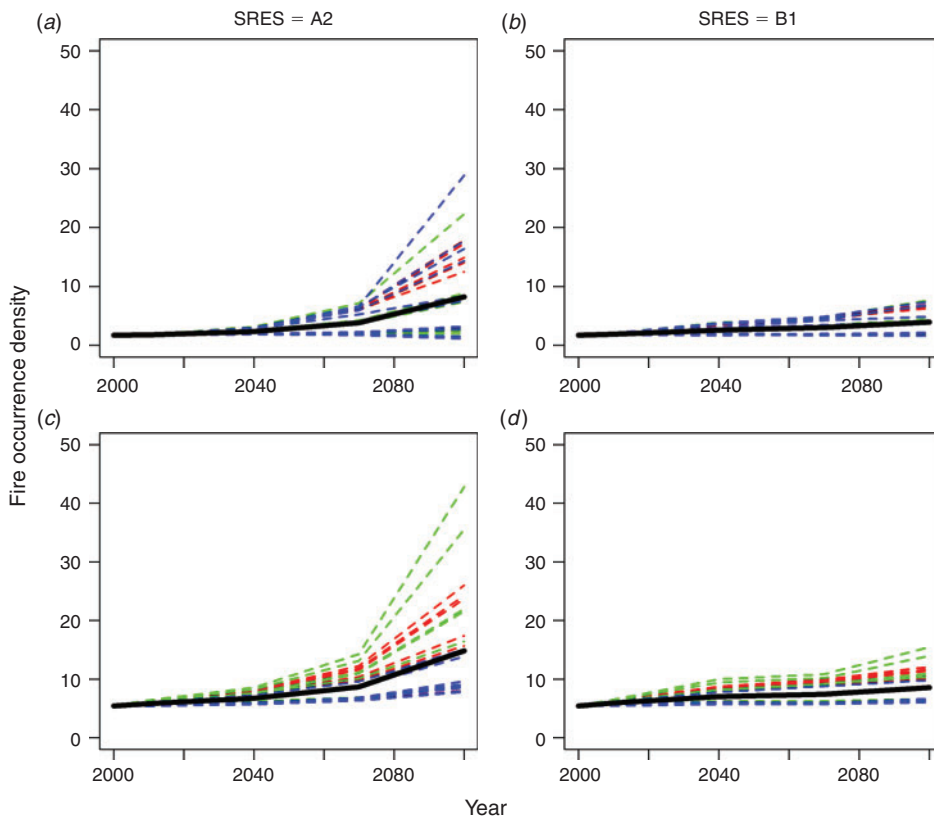


**Fig. 4.** Landscape-scale mean fire density predicted by the top 30 Poisson point process models under the climate scenario of SRES A2 and B1 for lightning-caused (*a* and *b*) and human-caused (*c* and *d*) fires. The unit of fire density is number of fires per 100 km$^2$ per decade. Each dashed line represents one model, with red, green and blue (for colour, refer to the online version of this paper, available at http://www.publish.csiro.au/) indicating the ranking order ($r > G > B$) of each model's weight of evidence. The black solid line represents the model averaging results.
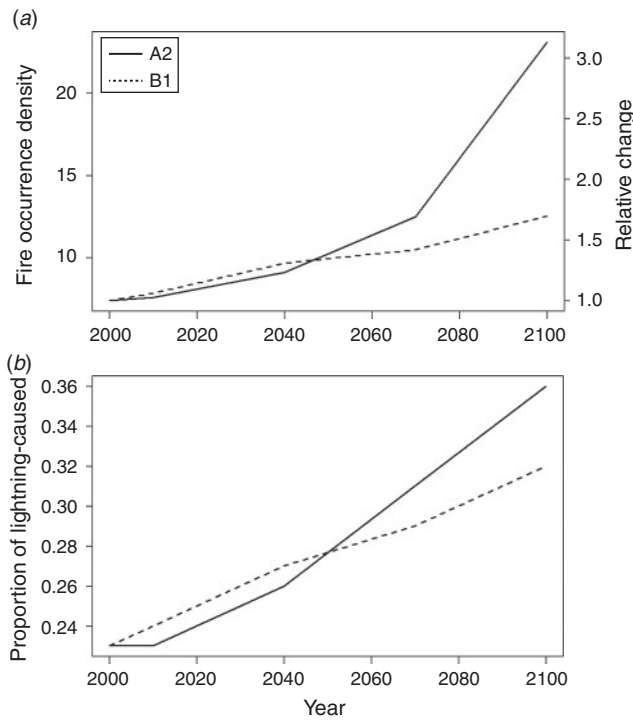
**Fig. 5.**  Predicted landscape-scale mean total (human-caused + lightning-caused) fire occurrence densities (fires per 100 km² per decade) and their relative changes under the SRES climate A2 and B1 scenarios (*a*), and time series of predicted proportion of lightning-caused fire occurrences (*b*).



**Fig. 6.**  Predicted landscape-scale mean total (human-caused + lightning-caused) wildfire occurrence density (number of fires per 100 km² per decade) at year 2000 (*a*) and year 2100 (*b*) under the SRES A2 scenario.

(Fig. 4), as predictor variables identified in each model and their corresponding parameters differed greatly (details in Table S1 and Table S2 in the Supplementary Material available online only at http://www.publish.csiro.au/?act=view_file&file_id=WF14001_AC.pdf). For lightning-caused wildfires, the predicted fire occurrence density at year 2100 under the SRES A2 scenario could reach as high as 28 fires per $10^6$ ha per decade (~16 times the current level of 1.7 fires per 100 km² per decade) or as low as 70% of the current level (Fig. 4*a*). Although the top 30 models were within 4 AIC units of each other, indicating similar weights of evidence, the range of their predictions was very large (70–1600% of the current level), suggesting high uncertainty when using a model selection approach to choose a single best model for predicting future conditions. The model averaging approach produced a more robust lightning-caused fire occurrence density at year 2100 under A2 scenario at 8.2 fires per 100 km² per decade, ~480% of the current level.

The range of predictions for human-caused fires at year 2100 was also large, varying from 140 to 720% of its current density. However, such uncertainty was much less than for predicted lightning-caused fires. The mean human-caused fire density at year 2100 under the A2 scenario was 14.8 fires per 100 km² per decade, ~260% of the current level (Fig. 4*c*). Both the range and mean of predicted fire occurrence density under the B1 scenario were lower than that under the A2 scenario in modelling lightning-caused (Fig. 4*b*) and human-caused (Fig. 4*d*) fires.

The predicted total fire occurrence density was then calculated as the sum of the predicted model-averaged human- and lightning-caused fires. The mean landscape total fire occurrence
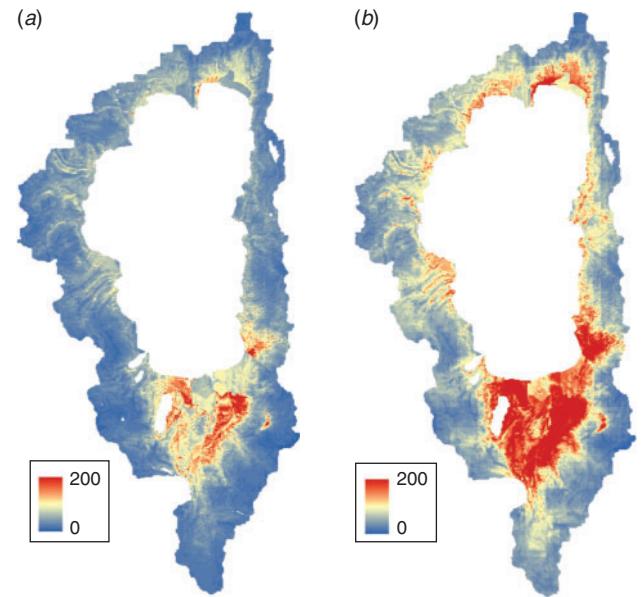
density was forecasted to increase to 170% of the current level under the B1 scenario and 310% under the A2 scenario. Further, the relative increase of lightning-caused fires was much greater than for human-caused fires. The proportion of lightning-caused fire occurrences was predicted to increase by 24–36% under the A2 scenario (Fig. 5). Consequently, the spatial patterns of fire occurrence hotspots (i.e. places with high fire occurrence density) under future climate scenarios were more influenced by the topographical variables (e.g. land form, elevation) that had stronger effects on lightning-caused fires. For example, areas that currently have a smaller fire risk, such as the north shore, east shore and higher ridge lines on the west shore of the LTB, might become fire occurrence hotspots in the future (Fig. 6) due to the predicted increase of lightning-caused fires.

## Discussion

### Environmental influences on wildfire occurrence patterns in LTB

Occurrence probability of any wildfire is a function of ignition source, topography, vegetation and climate. However, our study showed that the relative importance and influences of these spatial controls on wildfire occurrence differed between human- and lightning-caused fires (Fig. 3). Human-caused wildfires occurred with greater probability in places with high population density (e.g. South Lake Tahoe) and close to roads that are characterised by abundant human ignition sources and easy accessibility. Importance values and effect sizes for climatic variables were lower than for anthropogenic variables. This finding is in accordance with studies of human-caused wildfires in other regions (e.g. Yang *et al.* 2007; Syphard *et al.* 2008).

Lightning-caused wildfires in LTB were more probable in high elevation (high ridge lines of west) and relatively dry areas (e.g. west shore) with ample lightning strikes (Fig. 2). Many

forest landscapes of the western US experience frequent lightning strikes. Whether or not these lightning strikes can turn into wildfire occurrences depends on fuel conditions (e.g. fuel moisture) and the amount of precipitation that comes with the thunderstorms. Storms that produce lightning-caused fires are associated with greater instability and higher dew point depression (drier air) than storms that produce the most lightning strikes (Rorig and Ferguson 1999; Skinner *et al.* 2006). Topography can play an important role in determining convection process and precipitation patterns. The interaction of atmospheric processes and topography has strongly influenced spatial patterns of lightning-caused wildfires in LTB.

### Potential response of wildfire occurrence to climate change

Although both human- and lightning-caused fire frequencies were predicted to increase in warmer and drier future climate conditions, our SPP modelling showed a higher proportion of lightning-caused wildfire occurrences compared with human-caused wildfire occurrences in the predicted future LTB (Fig. 5). This was mainly because modelled climatic variables (e.g. climatic water deficit) were more strongly associated with lightning- than human-caused wildfires. Because lightning strikes are well distributed throughout the LTB, future warming and drying climate could greatly increase lightning-caused wildfires. In contrast, human-caused fires, even if they would increase in number, are mostly confined to the places where people are – mainly in urban areas and along roads with easy access. The significance of the change in spatial patterns is the occurrence of lightning-caused wildfires in places without easy access.

Our modelling approach used only 30-year average climates to represent climatic effects and did not incorporate key atmospheric processes that operate over shorter periods. Therefore, model outputs are most useful for describing potential trends and should not be interpreted as precise predictions. For example, increasing temperature may lead to changes in lightning density or to increased frequency of dry lightning, which would influence our predictions in ways that our model cannot account for. In addition, because we excluded the majority of small (10 ha) wildfires from the analysis, the model may underestimate future wildfire probability even for large wildfires, because of the potential for more fires that would remain small in today's climatic regime to become large in the future climate regime due to warmer climate and greater fuel availability.

The predicted climate change effects on spatial patterns of wildfire occurrence may be further altered by anthropogenic processes such as increasing recreation around the study area, as well as the active fuel management and fire suppression. In addition, wildfires may become self-limiting due to reduced fuel loads. Other modelling limitations include (1) assuming constant human infrastructures (e.g. roads and towns) and population densities over time, (2) lack of consideration for how wildfires may change landscape patterns of fuels by shifting dominant vegetation types and how such changes could alter fire regimes, and (3) lack of consideration for how other natural disturbances such as insect outbreaks could interact with wildfire in a climate change context (Kulakowski *et al.* 2013). These limitations are commonly acknowledged in studies that use statistical modelling of fire occurrences to make inferences of future spatial patterns (e.g. Krawchuk *et al.* 2009). Despite these limitations, our predictions can still provide a baseline to understand response of wildfire occurrence to climate change in LTB, as its overall trend (direction and magnitude) is consistent with other large-scale wildfire occurrence modelling studies, even though most of those studies used GLM rather than SPP models (e.g. Syphard *et al.* 2008; Miranda *et al.* 2012).

### Uncertainty in SPP modelling and prediction

To our knowledge, this study is the first attempt to conduct SPP data analysis within a model averaging framework for modelling spatial distribution of fire occurrences. SPP modelling has been increasingly applied for predicting responses of wildfire occurrences to climate change (e.g. Liu *et al.* 2012), but little is known about how the choice of model selection could affect prediction uncertainty. In this study, we found that multiple SPP models with similar model support led to substantially different predictions (Fig. 4). Such high levels of model uncertainty demonstrate the need to employ multi-model inference approaches when analysing historical wildfire occurrence data and predicting future fire occurrence in response to climate change.

Although integrating SPP with a model averaging approach is promising for obtaining the range and variation of predicted wildfire occurrence response to climate change, there are other sources of uncertainty such as choice of different model types (e.g. GLM *v.* SPP *v.* MaxENT), spatial accuracy of occurrence locations and lack of agreement in future climate conditions predicted by different climate models under various carbon emission scenarios. Our results indicate large differences of predicted landscape-level mean wildfire occurrence density between SRES A2 and B1 scenarios (Fig. 4), suggesting carbon emission scenarios and global climate models may exert greater influences on prediction uncertainty than SPP models. Therefore, comprehensive uncertainty analysis is warranted in future studies to better estimate wildfire occurrence changes over time in order to evaluate long-term effectiveness of fuel management plans.

### Management implications

It has been increasingly recognised that strategic planning of fuel management should be based on burn probability and fire risk assessment (Finney 2005; Miller *et al.* 2008; Liu *et al.* 2013). Recent studies on the effectiveness of fuel breaks in controlling large wildfires have demonstrated that a substantial proportion of the fuel breaks never intersected a fire over a long period (Syphard *et al.* 2011*a*). Therefore, mapping where fires are most likely to burn on the landscape could be part of the planning process to increase efficiency of new construction of fuel breaks. Spatial variability of wildfire occurrence plays an important role in burn probability mapping (Yang *et al.* 2008; Parisien *et al.* 2011). However, such spatial variability may be altered over time due to climate change. This change in distribution of wildfire occurrence hotspots poses a serious challenge to predicting the effectiveness of fuel treatment plans because the realised effectiveness of fuel treatment ultimately depends on the likelihood of a wildfire burning into treated areas

(Syphard *et al.* 2011*b*). It is important to incorporate such hot-spot information in long-term fuel treatment planning.

Fuel treatment in LTB has been mainly conducted in the WUI, where human-caused wildfires are pervasive. However, our study showed that wildfire occurrence hotspots in future LTB could shift to higher elevations and ridge tops (Fig. 6) as a result of faster increase in lightning-caused fires. Therefore, future fuel treatment may become necessary in those areas. Long-term fuel treatment planning should consider not only current landscape patterns of wildfire occurrence but also future patterns. Several studies have used forest landscape succession and disturbance simulation models such as LANDSUM and LANDIS-II to evaluate alternative long-term fuel treatment plans (e.g. Keane *et al.* 2011; Loudermilk *et al.* 2013). Those simulation modelling applications have begun to integrate both current and future spatial variability of fire occurrences in simulating dynamic fire regimes and its interaction with forest succession. Such integration further highlights the research needed to better predict fire occurrence distribution given both current and future climate conditions.

## Acknowledgements

## References

Baddeley A, Turner R (2000) Practical maximum pseudolikelihood for spatial point patterns. *Australian & New Zealand Journal of Statistics* **42**(3), 283–322. doi:10.1111/1467-842X.00128

Bailey TC, Gatrell AC (1995) 'Interactive Spatial Data Analysis.' (Longman Scientific & Technical: Harlow, UK)

Bar Massada A, Syphard AD, Hawbaker TJ, Stewart SI, Radeloff VC (2011) Effects of ignition location models on the burn patterns of simulated wildfires. *Environmental Modelling & Software* **26**(5), 583–592. doi:10.1016/J.ENVSOFT.2010.11.016

Burnham KP, Anderson DR (2002) 'Model Selection and Multi-model Inference: a Practical Information-theoretic Approach.' (Springer: New York, NY)

Diggle PJ (1983) 'Statistical Analysis of Spatial Point Patterns.' (Oxford University Press: London, UK)

Finney MA (2005) The challenge of quantitative risk analysis for wildland fire. *Forest Ecology and Management* **211**, 97–108. doi:10.1016/J.FORECO.2005.02.010

Finney MA (2007) A computational method for optimising fuel treatment locations. *International Journal of Wildland Fire* **16**(6), 702–711. doi:10.1071/WF06063

Finney MA, McHugh CW, Grenfell IC, Riley KL, Short KC (2011) A simulation of probabilistic wildfire risk components for the continental United States. *Stochastic Environmental Research and Risk Assessment* **25**(7), 973–1000. doi:10.1007/S00477-011-0462-Z

Flannigan MD, Krawchuk MA, de Groot WJ, Wotton BM, Gowman LM (2009) Implications of changing climate for global wildland fire. *International Journal of Wildland Fire* **18**(5), 483–507. doi:10.1071/WF08187

Grueber CE, Nakagawa S, Laws RJ, Jamieson IG (2011) Multimodel inference in ecology and evolution: challenges and solutions. *Journal of Evolutionary Biology* **24**(4), 699–711. doi:10.1111/J.1420-9101.2010.02210.X

Johnson JB, Omland KS (2004) Model selection in ecology and evolution. *Trends in Ecology & Evolution* **19**(2), 101–108. doi:10.1016/J.TREE.2003.10.013

Juan P, Mateu J, Saez M (2012) Pinpointing spatio-temporal interactions in wildfire patterns. *Stochastic Environmental Research and Risk Assessment* **26**(8), 1131–1150. doi:10.1007/S00477-012-0568-Y

Keane RE, Cary GJ, Flannigan MD (2011) Challenges and needs in fire management: a landscape simulation modeling perspective. In 'Landscape ecology in forest management and conservation: challenges and solutions for global change'. (Eds Chao Li, Raffaele Lafortezza, Jiquan Chen) pp. 75–98. (Higher Education Press: Beijing, China and Springer: Berlin Heideberg)

Kelly R, Chipman ML, Higuera PE, Stefanova I, Brubaker LB, Hu FS (2013) Recent burning of boreal forests exceeds fire regime limits of the past 10 000 years. *Proceedings of the National Academy of Sciences of the United States of America* **110**(32), 13055–13060. doi:10.1073/PNAS.1305069110

Krawchuk MA, Moritz MA (2011) Constraints on global fire activity vary across a resource gradient. *Ecology* **92**(1), 121–132. doi:10.1890/09-1843.1

Krawchuk MA, Moritz MA, Parisien MA, Van Dorn J, Hayhoe K (2009) Global pyrogeography: the current and future distribution of wildfire. *PLoS ONE* **4**(4), e5102. doi:10.1371/JOURNAL.PONE.0005102

Kulakowski D, Matthews C, Jarvis D, Veblen TT (2013) Compounded disturbances in sub-alpine forests in western Colorado favour future dominance by quaking aspen (*Populus tremuloides*). *Journal of Vegetation Science* **24**(1), 168–176. doi:10.1111/J.1654-1103.2012.01437.X

Liu Z, Yang J, Chang Y, Weisberg PJ, He HS (2012) Spatial patterns and drivers of fire occurrence and its future trend under climate change in a boreal forest of Northeast China. *Global Change Biology* **18**(6), 2041–2056. doi:10.1111/J.1365-2486.2012.02649.X

Liu Z, Yang J, He HS (2013) Studying the effects of fuel treatment based on burn probability on a boreal forest landscape. *Journal of Environmental Management* **115**, 42–52. doi:10.1016/J.JENVMAN.2012.11.004

Loudermilk EL, Scheller RM, Weisberg PJ, Yang J, Dilts TE, Karam SL, Skinner C (2013) Carbon dynamics in the future forest: the importance of long-term successional legacy and climate–fire interactions. *Global Change Biology* **19**(11), 3502–3515.

Lutz JA, van Wagtendonk JW, Franklin JF (2010) Climatic water deficit, tree species ranges, and climate change in Yosemite National Park. *Journal of Biogeography* **37**(5), 936–950. doi:10.1111/J.1365-2699.2009.02268.X

Maurer EP (2007) Uncertainty in hydrologic impacts of climate change in the Sierra Nevada, California, under two emissions scenarios. *Climatic Change* **82**(3–4), 309–325. doi:10.1007/S10584-006-9180-9

McCune B, Keon D (2002) Equations for potential annual direct incident radiation and heat load. *Journal of Vegetation Science* **13**(4), 603–606. doi:10.1111/J.1654-1103.2002.TB02087.X

Miller C, Parisien MA, Ager AA, Finney MA (2008) Evaluating spatially-explicit burn probabilities for strategic fire management planning. *Transactions on Ecology and the Environment* **19**, 245–252. doi:10.2495/FIVA080251

Miranda BR, Sturtevant BR, Stewart SI, Hammer RB (2012) Spatial and temporal drivers of wildfire occurrence in the context of rural development in northern Wisconsin, USA. *International Journal of Wildland Fire* **21**(2), 141–154. doi:10.1071/WF10133

Parisien MA, Moritz MA (2009) Environmental controls on the distribution of wildfire at multiple spatial scales. *Ecological Monographs* **79**(1), 127–154. doi:10.1890/07-1289.1

Parisien M-A, Parks SA, Miller C, Krawchuk MA, Heathcott M, Moritz MA (2011) Contributions of ignitions, fuels, and weather to the spatial patterns of burn probability of a boreal landscape. *Ecosystems* **14**(7), 1141–1155. doi:10.1007/S10021-011-9474-2

Parisien M-A, Snetsinger S, Greenberg JA, Nelson CR, Schoennagel T, Dobrowski SZ, Moritz MA (2012) Spatial variability in wildfire probability across the western United States. *International Journal of Wildland Fire* **21**(4), 313–327. doi:10.1071/WF11044

Podur J, Martell DL, Csillag F (2003) Spatial patterns of lightning-caused forest fires in Ontario, 1976–1998. *Ecological Modelling* **164**(1), 1–20. doi:10.1016/S0304-3800(02)00386-1

PRISM (2007) Climatological normals, 1971–2000. The PRISM Group, Oregon State University, Corvallis, OR.

Renner IW, Warton DI (2013) Equivalence of MAXENT and Poisson point process models for species distribution modeling in ecology. *Biometrics* **69**(1), 274–281. doi:10.1111/J.1541-0420.2012.01824.X

Rorig ML, Ferguson SA (1999) Characteristics of lightning and wildland fire ignition in the Pacific Northwest. *Journal of Applied Meteorology* **38**(11), 1565–1575. doi:10.1175/1520-0450(1999)038<1565:COLAWF>2.0.CO;2

Rothermel RC (1983) How to predict the spread and intensity of forest and range fires. USDA Forest Service general technical report, vol. 143, Intermountain Forest and Range Experiment Station. (Ogden, UT)

Safford HD, Schmidt DA, Carlson CH (2009) Effects of fuel treatments on fire severity in an area of wildland–urban interface, Angora Fire, Lake Tahoe Basin, California. *Forest Ecology and Management* **258**(5), 773–787. doi:10.1016/J.FORECO.2009.05.024

Sappington J, Longshore KM, Thompson DB (2007) Quantifying landscape ruggedness for animal habitat analysis: a case study using bighorn sheep in the Mojave Desert. *The Journal of Wildlife Management* **71**(5), 1419–1426. doi:10.2193/2005-723

Skinner CN, Tayor A, Agee JK (2006) Klamath mountains bioregion. In 'Fire in California's Ecosystems'. (Eds Neil G Sugihara, Jan W van Wagtendonk, Kevin E Shaffer, JoAnn Fites-Kaufman, Andrea E Thode) pp. 170–194 (University of California Press: Berkeley CA).

Stephens SL, Ruth LW (2005) Federal forest-fire policy in the United States. *Ecological Applications* **15**(2), 532–542. doi:10.1890/04-0545

Stephenson N (1998) Actual evapotranspiration and deficit: biologically meaningful correlates of vegetation distribution across spatial scales. *Journal of Biogeography* **25**(5), 855–870. doi:10.1046/J.1365-2699.1998.00233.X

Stoyan D, Penttinen A (2000) Recent applications of point process methods in forestry statistics. *Statistical Science* **15**(1), 61–78.

Syphard AD, Radeloff VC, Keuler NS, Taylor RS, Hawbaker TJ, Stewart SI, Clayton MK (2008) Predicting spatial patterns of fire on a southern California landscape. *International Journal of Wildland Fire* **17**(5), 602–613. doi:10.1071/WF07087

Syphard AD, Keeley JE, Brennan TJ (2011*a*) Factors affecting fuel break effectiveness in the control of large fires on the Los Padres National Forest, California. *International Journal of Wildland Fire* **20**(6), 764–775. doi:10.1071/WF10065

Syphard AD, Scheller RM, Ward BC, Spencer WD, Strittholt JR (2011*b*) Simulating landscape-scale effects of fuels treatments in the Sierra Nevada, California, USA. *International Journal of Wildland Fire* **20**(3), 364–383. doi:10.1071/WF09125

Taylor AH (2004) Identifying forest reference conditions on early cut-over lands, Lake Tahoe Basin, USA. *Ecological Applications* **14**(6), 1903–1920. doi:10.1890/02-5257

Taylor A, Beaty R (2005) Climatic influences on fire regimes in the northern Sierra Nevada mountains, Lake Tahoe Basin, Nevada, USA. *Journal of Biogeography* **32**(3), 425–438. doi:10.1111/J.1365-2699.2004.01208.X

Thornthwaite CW, Mather JR (1955) The water balance. 'Publications in Climatology' 8, 1–104 (Drexel Institute of Technology: Centerton NJ).

Vaisala Global Atmospherics (2012) National Lightning Detection System. (Vaisala: Tucson, AZ).

Warton D, Aarts G (2013) Advancing our thinking in presence-only and used-available analysis. *Journal of Animal Ecology* **82**(6), 1125–1134. doi:10.1111/1365-2656.12071

Warton DI, Shepherd LC (2010) Poisson point process models solve the 'pseudo-absence problem' for presence-only data in ecology. *The Annals of Applied Statistics* **4**(3), 1383–1402. doi:10.1214/10-AOAS331

Weiss A (2001) Topographic position and landforms analysis. Conference poster for the 'ESRI International User Conference', 9–13 July 2001, San Diego, CA, pp. 200–200.

Westerling AL, Hidalgo HG, Cayan DR, Swetnam TW (2006) Warming and earlier spring increase western US forest wildfire activity. *Science* **313**(5789), 940–943. doi:10.1126/SCIENCE.1128834

Whelan RJ (1995) 'The Ecology of Fire.' (Cambridge University Press: Cambridge, UK)

Whittingham MJ, Stephens PA, Bradbury RB, Freckleton RP (2006) Why do we still use stepwise modelling in ecology and behaviour? *Journal of Animal Ecology* **75**(5), 1182–1189. doi:10.1111/J.1365-2656.2006.01141.X

Wotton B, Nock C, Flannigan M (2010) Forest fire occurrence and climate change in Canada. *International Journal of Wildland Fire* **19**(3), 253–271. doi:10.1071/WF09002

Yang J, He HS, Shifley SR, Gustafson EJ (2007) Spatial patterns of modern period human-caused fire occurrence in the Missouri Ozark Highlands. *Forest Science* **53**(1), 1–15.

Yang J, He HS, Shifley SR (2008) Spatial controls of occurrence and spread of wildfires in the Missouri Ozark Highlands. *Ecological Applications* **18**(5), 1212–1225. doi:10.1890/07-0825.1